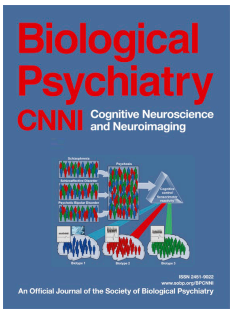

Intact Mismatch Negativity Responses in Clinical High-Risk for Psychosis and First-Episode Psychosis: Evidence from Source-Reconstructed Event-Related Fields and Time-Frequency Data

Pradeep Dheerendra, Ph.D., Tineke Grent-'t-Jong, Ph.D., Ruchika Gajwani, Ph.D., Joachim Gross, Ph.D., Andrew, I. Gumley, Ph.D., Rajeev Krishnadas, M.D., Ph.D., Stephen M. Lawrie, M.D., Matthias Schwannauer, Ph.D., Frauke Schultze-Lutter, Ph.D., Peter J. Uhlhaas, Ph.D.

PII: S2451-9022(23)00244-6

DOI: https://doi.org/10.1016/j.bpsc.2023.09.006

Reference: BPSC 1139

To appear in: *Biological Psychiatry: Cognitive Neuroscience and Neuroimaging*

Received Date: 23 June 2023

Revised Date: 26 August 2023

Accepted Date: 21 September 2023

Please cite this article as: Dheerendra P., Grent-'t-Jong T., Gajwani R., Gross J., Gumley A.,.I, Krishnadas R., Lawrie S.M, Schwannauer M., Schultze-Lutter F. & Uhlhaas P.J, Intact Mismatch Negativity Responses in Clinical High-Risk for Psychosis and First-Episode Psychosis: Evidence from Source-Reconstructed Event-Related Fields and Time-Frequency Data, *Biological Psychiatry: Cognitive Neuroscience and Neuroimaging* (2023), doi: https://doi.org/10.1016/j.bpsc.2023.09.006.

Number of Tables: 4

Number of Figures: 3

Number of Suppl. Figures: 4

Number of Suppl. Tables: 4

Intact Mismatch Negativity Responses in Clinical High-Risk for Psychosis and First-Episode Psychosis: Evidence from Source-Reconstructed Event-Related Fields and Time-Frequency Data

Dheerendra, Pradeep, Ph.D.[1], Grent-'t-Jong, Tineke, Ph.D.[1,2], Gajwani, Ruchika, Ph.D.[3], Gross, Joachim, Ph.D.[1,4], Gumley, Andrew, I., Ph.D.[3], Krishnadas, Rajeev, M.D., Ph.D.[1], Lawrie, Stephen M., M.D.[5], Schwannauer, Matthias, Ph.D.[6], Schultze-Lutter, Frauke., Ph.D.[7,8,9] & Uhlhaas, Peter J., Ph.D.[1,2]

1. School of Psychology and Neuroscience, University of Glasgow, Glasgow, U.K.
2. Department of Child and Adolescent Psychiatry, Charité Universitätsmedizin, Berlin, Germany
3. Mental Health and Wellbeing, Institute of Health and Wellbeing, University of Glasgow, Glasgow, U.K.
4. Institute for Biomagnetism and Biosignalanalysis, University of Muenster, Muenster, Germany
5. Department of Psychiatry, University of Edinburgh, Edinburgh, U.K.
6. Department of Clinical Psychology, University of Edinburgh, Edinburgh, U.K.
7. Department of Psychiatry and Psychotherapy, Medical Faculty, Heinrich Heine University Düsseldorf, Germany
8. Department of Psychology, Faculty of Psychology, Airlangga University, Surabaya, Indonesia
9. University Hospital of Child and Adolescent Psychiatry and Psychotherapy, University of Bern, Bern, Switzerland

Running Head title: MMN-Responses in CHR-Ps and FEPs

Keywords: Schizophrenia, Psychosis High Risk, Magnetoencephalography, Mismatch Negativity, Source-Reconstruction, Time-Frequency Analysis

Number of words of the Abstract: 167

Number of words of the manuscript: 3961

Correspondence:

Prof. Peter J. Uhlhaas

Department of Child and Adolescent Psychiatry

Augustenburger Platz 1

Charité Universitätsmedizin

Berlin 13353

Germany

Email: peter.uhlhaas@charite.de

Tel: +49 30 450 516 193

Abstract

Background: To examine whether Mismatch Negativity (MMN) Responses are impaired in participants at clinical high-risk for psychosis (CHR-P) and first episode psychosis (FEP) patients and whether MMN-deficits predict clinical outcomes in CHR-Ps.

Methods: Magnetoencephalography (MEG) data were collected during a duration-deviant MMN-paradigm for a group of 116 CHR-P participants, 33 FEP patients, (15 antipsychotic-naïve), a psychosis-risk-negative group (CHR-N: n=38) with substance abuse and affective disorder and 49 healthy controls (HC). Analysis of group differences of source-reconstructed event-related fields as well as time-frequency and inter-trial-phase-coherence (ITPC) focused on bilateral Heschl's gyri and superior temporal gyri.

Results: Significant MMNm responses were found across participants in bilateral Heschl's gyrus and superior temporal gyri. However, MMN-amplitude as well as time-frequency and ITPC-responses were intact in CHR-P and FEP-patients relative to HC. Furthermore, MMN-deficits were not related to persistent attenuated psychotic symptoms nor transitions to psychosis in CHR-Ps.

Conclusions: Our data suggest that MMNm responses in MEG-data are not impaired in early-stage psychosis and may not predict clinical outcomes in CHR-P participants.

Introduction

Mismatch negativity (MMN) is an event-related potential/field (ERP/ERF) elicited when the brain detects a random violation of an established pattern of sensory input (1). Auditory MMN-generators have been localized in the superior temporal gyri as well as frontal regions (2) and have been shown to depend on N-methyl-D-aspartate (NMDA) receptor mediated glutamatergic transmission (3).

Several models have been proposed to explain the generation of MMN-responses, such as the predictive coding framework (2, 4, 5) and passive adaption to repeated stimuli (6-8). Passive adaptation models of MMN responses account for deviant responses in terms of an oscillatory or rebound response. However, the MMN-response to omitted sounds is more difficult to accommodate within this model (9, 10).

In schizophrenia (ScZ)-patients, MMN amplitudes and its neuromagnetic counterpart MMNm have been consistently found to be reduced (11), correlate with impaired social functioning (12, 13), cognitive deficits (14), and reductions in grey matter (15). In addition, several studies have examined whether MMN-deficits are present in early-stage psychosis. Clinical high-risk for psychosis (CHR-P) criteria have been developed based on the presence of attenuated psychotic symptoms (APS) (16, 17) as well as in relationship to the basic symptom (BS) concept proposed by Huber and colleagues (18). Overall, approx. 22% of CHR-P participants will develop a first-episode of psychosis (FEP) within a 3-year period (19).

Several studies have reported MMN deficits in CHR-Ps (20-39), while other studies have reported intact MMN-responses (40-47). Moreover, there is evidence that reduced MMN-responses predict transition to psychosis in CHR-P participants (48) (but see (22, 40)) as well as persistence of APS (29) and functional outcomes (21). Meta-analytic evidence suggests that MMN responses to pitch-deviants are not impaired in FEPs while duration deviants are associated with a small-to-medium effect size (Cohen's d = 0.47) (11).

More recently, impaired MMN-responses have been linked to deficits in neural oscillations (49). Specifically, it has been proposed that MMN generation primarily reflects activity in theta (4-7Hz) frequency band (50), and that the MMN component involves an oscillatory phase reset characterized by increased intertrial phase coherence (ITPC) (51). However, there is also evidence for the contribution of alpha-band oscillations in the

encoding of standard stimuli (52). Currently, it is unclear, however, whether neural oscillations are impaired during MMN-processing in CHR-Ps (33).

To address whether MMN responses and the associated oscillatory components are impaired in early-stage psychosis, we applied a state-of-the-art MEG approach in a sample of CHR-Ps (n = 116) as well as FEP-patients (n = 33). In addition, we recruited 38 participants with substance abuse and affective disorder (clinical high-risk negative, CHR-N) as well as a group of healthy controls (n = 49). MEG-data were analysed at both sensor- and source-level for MMN amplitude, spectral power, and intertrial-phase coherence (ITPC) and correlated with clinical and neurocognitive variables (43). We predicted that FEP and CHR-P participants would be characterized by a reduction in both MMNm amplitude as well as decreased low-frequency spectral-power and deficient ITPC responses in auditory regions given the existing findings in ScZ-patients (33, 52), which would be closely linked to clinical outcomes in CHR-Ps.

Methods and Materials

Participants

A total of 236 participants were recruited as part of the Youth Mental Health Risk and Resilience study (YouR) (53). CHR-P participants were recruited from the general community through an online-screening approach (54). Study participants were divided into the following groups: 1) 116 participants that met CHR-P criteria, (2) 38 participants characterized by non-psychotic disorders, viz. affective disorders (n=11), anxiety disorders (n=16), eating disorders (n=1), and/or substance abuse (n=10) (CHR-N), 3) 33 patients with FEP (15 antipsychotic-naïve) and, 4) 49 healthy controls (HC) without an axis I diagnosis or family history of psychosis.

CHR-P status was established according to ultra-high risk criteria of the Comprehensive Assessment of At Risk Mental States (CAARMS) Interview (16) and the Cognitive Disturbances (COGDIS) and Cognitive-Perceptive (COPER) basic symptoms criteria, Schizophrenia Proneness Instrument, Adult version (SPI-A) (55). The Structured Clinical Interview for DSM-5 (SCID) (56) were used to assess FEP patients and the Positive and Negative Symptom Scale (PANSS) (57) was employed to assess current psychopathology. For all groups except FEP-patients, cognition was assessed with the Brief Assessment of Cognition in Schizophrenia (BACS) (58) (see Tables 1-3).

The study was approved by the ethical committees of University of Glasgow and the NHS Research Ethical Committee Glasgow & Greater Clyde. All participants provided written informed consent.

INSERT_TABLE_1

INSERT_TABLE_2

INSERT_TABLE_3

Clinical Follow-Up

CHR-P participants were re-assessed at regular intervals (3, 6, 9, 12, 18, 24, 30 and 36 months) to examine persistence of attenuated psychotic symptoms (APS) up to 12 months and transition to psychosis (see Supplement, and Table S1).

Stimuli and Task

Auditory stimuli trains consisting of sequences of 5 harmonic tone complexes consisting of 440 Hz and 880 Hz sinusoids were presented. The tones in the standard (STD) sequence were 80 ms in duration with 7 ms ascending and descending ramps and a 150 ms sound onset asynchrony between consecutive tones within a sequence and were presented with 60% probability. Deviant (DEV) sequences contained a duration deviant tone of 40 ms at the last position and were presented with 20% probability. The 5th tone was omitted in 20% of sequences but the results are not reported here. The inter sequence interval (ISI) were randomly jittered between 700 to 1000 ms. All sounds were presented at the default sound level of 81 dB unless a participant's hearing was impaired (increased sound level to 93 dB) or too sensitive (decreased to 71 dB).

The auditory stimuli were presented in three blocks, each block consisting of 200 trials and lasting approximately five minutes. The trials were presented in pseudorandomized order so that each block started with three standard sequences before delivering the first deviant/omission sequence and two deviant sequences were never presented consecutively. The auditory stimuli were presented binaurally via MEG-compatible 6-meter-long plastic tubes attached to earplugs using an Etymotic ER-30 system (Etymotic Research, Inc. United States of America). The MEG tasks were presented using Presentation® software (Version 18.0, Neurobehavioral Systems, Inc., Berkeley, CA).

INSERT_FIGURE_1

Visual letter detection task

The auditory paradigm was combined with a visual letter detection task to control for differences in attention. The visual stimuli consisted of 20 target letters (X) among 100 non-target letters (R, S, T, U, V, W, Y, Z) that were pseudo-randomly interspersed within the auditory series. Visual stimuli were always presented during

standard trials and were time-locked to the presentation of the first sound with an onset jitter difference between auditory and visual stimulation of 10-90 ms (in 10 ms steps), and a duration of 150 ms. Visual targets were always presented during extra inserted standard trials that were removed for further analyses. The font-size was increased when necessary for participants with poor vision. Viewing distance was approximately 80 cm.

Neuroimaging

MEG-data were acquired at baseline from a 248-channel 4D-BTI magnetometer system (MAGNES® 3600 WH, 4D-Neuroimaging, San Diego), recorded at 1017.25 Hz sampling rate, with online low pass filter of 400 Hz pass band. Prior to the MEG-recording, the head-shape and five head position indicator (HPI) coils were digitized using a Polhemus Fastrack digitizer. Head position was recorded at the beginning and the end of each block. For subject-specific source localization of MEG activity, T1 anatomical scans (3D MPRAGE sequences) were collected on a Siemens Trio Tim 3T-scanner (192 slices, voxel size 1 mm^3, FOV=256x256x176 mm^3, TR=2250 ms, TE=2.6 ms, FA=9°).

MEG Data Analysis

MEG data were analysed with MATLAB (2020b; The MathWorks, Inc., Natick, MA) using the open-source FieldTrip Toolbox version 20201201 (http://www.fieldtriptoolbox.org/). Continuous MEG data were epoched into 2000 ms (700 ms pre-stimulus to 1300 ms post-stimulus) segments, filtered to remove power-line noise (50, 100, 150 Hz) using a discrete 50 Hz Fourier transform filter. Faulty sensors with large signal variance or flat signals were removed and data were downsampled to 250 Hz. Artifact-free data were created by removing trials with excessive transient muscle activity, slow drift, or superconducting quantum interference device jumps using visual inspection and applying independent component analysis (ICA) based detection and removal of components containing eye blink, eye movement, and electrocardiographic artifacts from the MEG signals.

Evoked response fields (ERF) were computed on -0.7s to 1.3s long epochs, low pass filtered at 20 Hz using fourth order Butterworth infinite impulse response (IIR) filter two pass-reverse, and baseline corrected (-200

to 0 ms). For sensor level analyses, ERF data were transformed to planar gradient configuration using the nearest neighbour method to facilitate the topographical interpretation of the data. The duration MMNm response was computed by subtracting the waveform of the standard sequence from the waveform of the deviant sequence. Latencies of MMNm response refer to the onset of the first tone of the sequence of five tones rather than the onset of deviant tone (600 ms).

MEG Source analysis

The main analyses focused on data transformed into source space because regional specificity at each sensor is compromised by field spread through inputs from multiple sources and interindividual differences in temporal cortex folding (59). The basic source level analysis steps included the following: (1) identification of regions activate during MMNm response and (2) analyses of subset of these regions for main group effects (HC, CHR-N, CHR-P, FEP).

MEG data were co-registered with the individual T1 MRI scans, using anatomical landmarks (nasion, bilateral preauricular points) and head-shape data collected using a Polhemus 3D Fasttrack digitization system (Polhemus, Colchester, VT) , followed by an automatic co-registration procedure with the ICP algorithm (60). A single-shell volume conductor model was utilized for individual head models. The head model was further warped into a three-dimensional template grid (5 mm resolution grid) in Montreal neurological institute (MNI) coordinates to normalize the source position and reduce individual differences.

Whole brain source localisation of evoked responses was performed using Linearly Constrained Minimum Variance (LCMV) beamformer implemented in Fieldtrip. LCMV beamformer estimates weights that linearly map the MEG sensors to source space. Sources were estimated for both conditions using common filter weights, thus ensuring that differences in source activity were not related to spatial filter differences. Twenty Hz low pass filtered evoked responses between 765 to 785 ms post onset of tone sequence (i.e. 165-185 ms post onset of the last tone in the sequence) for both conditions in all participants were inverted using this common filter approach.

Source-space (virtual electrode) data were extracted for each voxel of a ROI defined in Automated Anatomical Labelling (AAL) atlas using the BrainNet Viewer software (61), followed by warping into individual

normalized MRI to extract signals at a brain region. The LCMV beamformer was used to compute the source-space data with the covariance matrix based on the time window from -700 to 1300 ms. The regularization value of the covariance matrix was set to 5%. Finally, time series computed separately for each voxel within a ROI were then combined into one time series per ROI using the singular value decomposition (SVD) component across the single-voxel data, which represents the dominant source orientation.

To assess potential condition and group differences in duration MMNm amplitudes, artifact-free virtual channel time-series were extracted at four pre-specified ROIs for each participant. Selected ROIs were defined for the left and right Heschl's gyri (HES), and superior temporal gyri (STG) based on the AAL atlas. The selection of these ROIs was based on source localization results of the same data across participants from all groups. Absolute values were used to avoid cancellation across trials due to arbitrary signs and thus possible opposite polarities.

Time Frequency representation

Time-frequency representations (TFRs) were computed on timeseries extracted from each virtual electrode separately using the multi-taper-method convolution algorithm implemented in Fieldtrip with Hanning tapers ranging from 1 to 30 Hz with a sliding 500-ms time-window, in step size of 10 ms and frequency resolution of 0.25 Hz. Corresponding intertrial phase coherence (ITPC) activity was computed from Fourier output. All data were expressed as a relative change (relch) from baseline activity (−400 to 0 ms).

Statistical Analyses

To evaluate sensor-level MMNm responses, ERFs were averaged between 765 ms to 785 ms post onset of the first tone in the sequence (i.e. 165 to 185 ms post onset of the deviant tone or MMNm time window) and subjected to a non-parametric Monte-Carlo permutation based (n=1000 random draws) dependent sample t-test (α=0.025, one sided, cluster-corrected) in Fieldtrip. To evaluate the main effect of group, a permutation-based (n=2000) F-test (α=0.05, cluster corrected) was conducted on the same data.

The cortical regions underlying MMNm response were identified via a permutation based (n=1000) dependent sample t-test (α=0.05, one-sided DEV > STD, FDR-corrected) using source activity in the MMNm time

window on entire cohort. The ROIs underlying main effect of condition (DEV>STD) were identified using a permutation based (n=2000) dependent sample t-test (α=0.05, FDR-corrected) on the difference in ERF for DEV and STD sequences averaged over MMNm time window. The ROIs underlying group differences in MMNm responses were identified using a permutation based (n=2000) F-test (α=0.05, FDR-corrected) on the same data.

An F-test was conducted on responses to standards in these ROIs to identify any group differences. Next, virtual electrodes showing differences in MMNm ERF response between groups (APS-P vs APS-NP; CHR-P-Transition vs CHR-P-No-Transition; FEP-Medicated vs FEP-Unmedicated) were identified using a permutation based (n=2000) independent sample t-test (α=0.025, two-sided, FDR-corrected) on ERF data averaged over MMNm time window.

The ROIs exhibiting main effect of condition (DEV > STD) in theta band power enhancement (or phase reset) were identified using a permutation based (n=2000) dependent sample t-test (α=0.05, FDR-corrected) on the difference in spectral power (or ITPC) between DEV and STD conditions averaged over 650 to 900 ms window post onset of the first tone in the tone sequence (i.e. 50 to 300 ms post onset of the last tone in the sequence) and 4 to 8 Hz frequency band. The ROIs underlying group differences were identified using a permutation based (n=2000) F-test (α=0.05, FDR-corrected) on this same data. A similar F-test was conducted on responses to standards in alpha (8-12 Hz) band in these ROIs to identify any group differences.

Next, virtual electrodes showing differences in MMNm theta band power (or phase reset) response between groups (APS-P vs APS-NP; CHR-P-Transition vs CHR-P-No-Transition; FEP-Medicated vs FEP-Unmedicated) were identified using a permutation based (n=2000) independent sample t-test (α=0.025, two-sided, FDR-corrected) on the difference in spectral power (or ITPC) between DEV and STD conditions averaged over 650 to 900 ms window post onset of the first tone in the tone sequence (i.e. 50 to 300 ms post onset of the last tone in the sequence) and 4 to 8 Hz frequency band.

Correlations of MMNm amplitude with cognitive and clinical measures in CHR-Ps

Stepwise linear regression was used to identify significant correlations between MMNm amplitudes (averaged over 20 ms around grand average peak MMN), BACS composite scores and individual subtests, APS severity as well as social and role global functioning scores in the CHR-P group.

Results

Demographic/Clinical Data and Task Performance

The FEP group had significantly more male participants than the HC ($p = 0.004$), CHR-N ($p = 0.002$), and CHR-P groups ($p < 0.001$) (Table 1). Patients with FEP were significantly older than CHR-Ps ($p = .015$). CHR-P participants had significantly fewer years of education ($p = 0.032$) and significantly lower BACS composite ($p = 0.014$), token motor ($p < 0.001$), and symbol coding ($p = 0.002$) scores than HC participants. The FEP, CHR-P, and CHR-N groups had significantly lower GAF scores than HCs and each other (all p values < 0.001). CHR-Ps group had also lower scores than the HC group in global role functioning ($p < 0.001$). Both CHR-P and CHR-N groups were also characterized by lower social functioning (CHR-N, $p = 0.003$; CHR-P, $p < 0.001$). Task performance i.e., accuracy and false alarm rates, were similar across groups. (Table 1).

Follow-up Outcomes

Follow-up data were available for 110 of the 116 CHR-P individuals (see Supplementary Material). Thirty-four CHR-P subjects continued to meet APS criteria at 12 months (APS-P), whereas 39 CHR-P subjects did not (APS-NP). The APS-P group scored significantly higher on CAARMS severity ($p = 0.001$) at baseline ($p = 0.028$) (Table S2) compared with APS-NPs. A total of 13 participants (11.2%) made a transition to psychosis (mean follow-up period: = 18 months) (Table S3). Compared to the CHR-P-NT group, transitioned CHR-P-T subjects had significantly lower GAF ($p = 0.034$) and GF social scores ($p = 0.023$) at baseline.

Sensor-level MMNm responses

Evoked responses to deviants were greater than for standards over right temporal sensors (Supplementary Figure 1) across all participants viz. $t(235) = 1927.3$ ($p < 0.002$, cluster corrected) during the MMNm interval in the entire sample as well as within each group independently showing a robust MMNm response. However, there was no main effect of group i.e. $F(3,232)$ values below 11.5, for any of the clusters (p-value = 0.55).

Source-level MMNm responses

A main effect of condition for MMN-responses was observed in bilateral auditory cortical regions, viz. Heschl's Gyrus and Superior Temporal Gyrus (Figure 1). A main effect of condition (DEV > STD) was found for evoked responses from all the 4 ROIs during MMNm window in the entire cohort viz. $t(235)$ values above 4.6, for any of the ROIs (p-values, 2e-6, 9e-6, 0, and 0 for LHES, LSTG, RHES, RSTG respectively). There were no group differences for evoked responses in these 4 ROIs (Table 4). In addition, there were no group differences in response to standards. There were no group differences for any of the clinical subgroup comparisons viz. APS-P vs. APS-NP; CHR-P Transitioned vs Non-Transitioned; FEP-Medicated vs FEP-UnMedicated patients (see Supplementary Table S4).

INSERT_FIGURE_2

INSERT_TABLE_4

Source-level spectral responses

A main effect of condition (DEV > STD) was found in theta (4-8) power and ITPC during the MMNm window (650-900 ms) in the entire cohort for all ROIs viz. theta power: $t(235)$ values above 6.4, for any of the ROIs (p-values, 9e-12, 8e-10, 0, and 0 for LHES, LSTG, RHES, RSTG respectively); theta ITPC: $t(235)$ values above 4.2, for any of the ROIs (p-values, 4e-5, 2e-5, 2e-10, and 8e-11 for LHES, LSTG, RHES, RSTG respectively). Similar to ERF-responses, there were no group differences in theta (4-8 Hz) power for MMN-

responses (Table 4, Supplementary Figure 3); alpha (8-12 Hz) response to standards. Moreover, ITPC-data also showed no group differences in theta band to MMNm (Table 4, Supplementary Figure 4) nor alpha band ITPC response to standards. There were no group differences for any of the clinical subgroup comparisons viz. APS-P vs. APS-NP; CHR-P Transitioned vs Non-Transitioned; FEP-Medicated vs FEP-UnMedicated patients (see Supplementary Table S5 for theta power and Table S6 for theta ITPC).

INSERT_FIGURE_3

Correlations of MMNm amplitude with cognitive and clinical measures in CHR-Ps

Stepwise linear regression between MMNm peak amplitudes in bilateral auditory cortices and CAARMS and SPI-A total scores, social and role global functioning in the CHR-P sample revealed no significant correlations. Processing speed was positively correlated with duration deviant MMNm peak amplitude in right Heschl's gyrus ($p = .031$), but it did not survive corrections for multiple comparisons, however.

Discussion

We examined MMN-responses during duration deviants in MEG-data in FEP- and CHR-P groups to investigate whether early-stage psychosis is characterized by impaired MMNm and corresponding spectral responses. In addition, we tested whether MMNm-data predicted clinical outcomes in CHR-Ps. Our results show that MMNm, spectral power as well as ITPC in CHR-P and FEPs were intact. Moreover, there were no robust relationships between MMNm-data and clinical outcomes in CHR-Ps.

MMNm responses were source localized to bilateral Heschl's gyrus and Superior Temporal Gyrus. This is consistent with prior findings (31, 33, 38) employing MEG that found MMNm-related activity in auditory cortical regions bilaterally (2). However, as in previous MEG-studies (31, 33, 38), we failed to detect frontal MMNm generators which has been reported in some EEG-analyses (62-64). One reason for the absence of frontal sources in our data could be the fact that MEG is not very sensitive to radially oriented generators (65).

In terms of group differences, MMNm responses were intact in CHR-Ps and FEP-groups. The absence of MMNm deficits in CHR-Ps is in agreement with previous findings (40-47) but see (20-38). As regards FEP-patients, some studies suggested also intact MMN (44, 66-71) while others observed impaired MMN-responses (22, 32, 34, 45, 72, 73). There was only modest evidence for a reduction in MMN-amplitudes in our data with the largest differences between FEP and HC seen in the left Heschl's gyrus which is consistent with prior findings (74) but these effects did not reach statistical significance. Our results are in agreement with a meta-analysis, suggesting that the size of MMN-deficits may not differ between CHR-Ps and FEP-schizophrenia patients (11), highlighting that pronounced impairments in MMN may only occur at later illness stages (74).

A novel aspect of our study is the investigation of spectral power and ITPC changes during MMN-responses in early-stage psychosis. Bilateral primary and secondary auditory cortices showed theta power enhancement and theta phase resetting during MMN responses as observed in previous studies (52). However, there were no deficits in theta/alpha-band responses to deviants and standards n in both FEPs and CHR-Ps. A recent study (33) that investigated MMN and spectral responses in MEG-data reported reduced MMNm responses in both

CHR-Ps and FEPs as well as a deficit in theta-band ITPC in CHR-Ps but these results did not survive correction for multiple comparisons, however.

Conflicting evidence exists whether reduced MMN-amplitudes in CHR-Ps can also predict clinical outcomes. EEG-measured MMN-responses predicted transition to psychosis in CHR-Ps (29, 30, 36, 45-47) as well as persistence of APS (29). However, other studies (22, 40, 42) did not confirm these findings, suggesting that the prognostic potential of MMN for predicting clinical outcomes in early-stage psychosis remains unclear. Consistent with this perspective, MMN-responses as well as spectral power and ITPC-correlates in our study did not predict transition to psychosis nor robustly persistence of APS. Thus, we could only observe trend-level effect between reduced MMN-responses and persistence of APS.

There are several potential variables that must be considered given the findings in our study. Firstly, we examined neuromagnetic MMN-responses whereas the majority previous studies examined EEG-data (20-30, 32, 34-37, 40-47). MEG and EEG differ in their sensitivity to the spatial orientation of the underlying generators. Whereas MEG is largely insensitive to radial sources, EEG is sensitive to all orientations, although the amount of cortex truly silent to MEG may be relatively small (65). Moreover, we previously demonstrated that MEG-recorded 40Hz Auditory Steady State Responses (ASSRs) (75) as well as during a visual grating task (76) were characterized by significant differences between CHR-Ps, FEPs and controls as well as predicted clinical outcomes in CHR-Ps.

Secondly, we recruited CHR-Ps who were self-referred from the general population. There is evidence to suggest that recruitment of CHR-Ps outside clinical pathways is associated with a dilution of psychosis-risk (77-80). Indeed, the number of transitions in our sample (11%) was somewhat lower than in previous clinical cohorts (19). However, we have also shown that CHR-P participants in our sample share many clinical and neurocognitive features than CHR-Ps recruited from clinical pathways (81). Moreover, a large study (46) with n = 580 CHR-Ps also showed no MMN deficit but only in those who later transitioned to psychosis.

Finally, the majority of previous MMN studies employed duration deviants that were longer in duration than standard tones (21-25, 27, 29-36, 38, 46, 47). In contrast, we employed deviants that were characterized by shorter tones than standards. Indeed, Atkinson, Michie (20) showed that the effect size of MMN deficit in CHR-Ps and FEPs was smaller for shorter compared to longer deviants.

Summary

Our findings show that MNNm as well as its spectral and ITPC correlates in CHR-P and FEP-patients are intact. Furthermore, MEG-responses in our study did not predict clinical outcomes in CHR-Ps. Taken together, our data suggests that deficient MMNm may not be a reliable biomarker for early-stage psychosis.

Disclosures and acknowledgments

Dr. Uhlhaas has received research support from Lilly and Lundbeck outside the submitted work. The study was supported by the Medical Research Council (MR/L011689/1). Dr. Rajeev Krishnadas was supported by the Neurosciences Foundation. Drs. Dheerendra, Grent-'t-Jong, Gajwani, Gross, Gumley, Lawrie, Schwannauer and Schultze-Lutter reported no biomedical financial interests or potential conflicts of interest.

We thank Frances Crabbe for help in the acquisition of MEG/MRI-data. The investigators also acknowledge the support of the Scottish Mental Health Research Network (http://www.smhrn.org.uk) now called the NHS Research Scotland Mental Health Network (NRS MHN: http://www.nhsresearchscotland.org.uk/research-areas/mental-health) for providing assistance with participant recruitment, interviews, and cognitive assessments. We would like to thank both the participants and patients who took part in the study and the research assistants of the YouR-study for supporting the recruitment and assessment of CHR-participants.

References

1. Naatanen R, Paavilainen P, Rinne T, Alho K (2007): The mismatch negativity (MMN) in basic research of central auditory processing: a review. *Clin Neurophysiol*. 118:2544-2590.
2. Garrido MI, Kilner JM, Stephan KE, Friston KJ (2009): The mismatch negativity: a review of underlying mechanisms. *Clin Neurophysiol*. 120:453-463.
3. Javitt DC, Steinschneider M, Schroeder CE, Arezzo JC (1996): Role of cortical N-methyl-D-aspartate receptors in auditory sensory memory and mismatch negativity generation: implications for schizophrenia. *Proc Natl Acad Sci U S A*. 93:11962-11967.
4. Wacongne C, Changeux JP, Dehaene S (2012): A neuronal model of predictive coding accounting for the mismatch negativity. *J Neurosci*. 32:3665-3678.
5. Lieder F, Daunizeau J, Garrido MI, Friston KJ, Stephan KE (2013): Modelling trial-by-trial changes in the mismatch negativity. *PLoS Comput Biol*. 9:e1002911.
6. May P, Tiitinen H, Ilmoniemi RJ, Nyman G, Taylor JG, Naatanen R (1999): Frequency change detection in human auditory cortex. *J Comput Neurosci*. 6:99-120.
7. May PJ, Westo J, Tiitinen H (2015): Computational modelling suggests that temporal integration results from synaptic adaptation in auditory cortex. *Eur J Neurosci*. 41:615-630.
8. May PJ, Tiitinen H (2010): Mismatch negativity (MMN), the deviance-elicited auditory deflection, explained. *Psychophysiology*. 47:66-122.
9. Wacongne C, Labyt E, van Wassenhove V, Bekinschtein T, Naccache L, Dehaene S (2011): Evidence for a hierarchy of predictions and prediction errors in human cortex. *Proc Natl Acad Sci U S A*. 108:20754-20759.
10. Salisbury DF (2012): Finding the missing stimulus mismatch negativity (MMN): emitted MMN to violations of an auditory gestalt. *Psychophysiology*. 49:544-548.
11. Erickson MA, Ruffle A, Gold JM (2016): A Meta-Analysis of Mismatch Negativity in Schizophrenia: From Clinical Risk to Disease Specificity and Progression. *Biol Psychiatry*. 79:980-987.
12. Hermens DF, Ward PB, Hodge MA, Kaur M, Naismith SL, Hickie IB (2010): Impaired MMN/P3a complex in first-episode psychosis: cognitive and psychosocial associations. *Prog Neuropsychopharmacol Biol Psychiatry*. 34:822-829.
13. Light GA, Braff DL (2005): Mismatch negativity deficits are associated with poor functioning in schizophrenia patients. *Arch Gen Psychiatry*. 62:127-136.
14. Baldeweg T, Klugman A, Gruzelier J, Hirsch SR (2004): Mismatch negativity potentials and cognitive impairment in schizophrenia. *Schizophr Res*. 69:203-217.
15. Dietsche B, Kircher T, Falkenberg I (2017): Structural brain changes in schizophrenia at different stages of the illness: A selective review of longitudinal magnetic resonance imaging studies. *Aust N Z J Psychiatry*. 51:500-508.
16. Yung AR, Yuen HP, McGorry PD, Phillips LJ, Kelly D, Dell'Olio M, et al. (2005): Mapping the onset of psychosis: the Comprehensive Assessment of At-Risk Mental States. *Aust N Z J Psychiatry*. 39:964-971.
17. Miller TJ, McGlashan TH, Rosen JL, Cadenhead K, Cannon T, Ventura J, et al. (2003): Prodromal assessment with the structured interview for prodromal syndromes and the scale of prodromal symptoms: predictive validity, interrater reliability, and training to reliability. *Schizophr Bull*. 29:703-715.
18. Schultze-Lutter F, Ruhrmann S, Fusar-Poli P, Bechdolf A, Schimmelmann BG, Klosterkotter J (2012): Basic symptoms and the prediction of first-episode psychosis. *Curr Pharm Des*. 18:351-357.
19. Fusar-Poli P, Salazar de Pablo G, Correll CU, Meyer-Lindenberg A, Millan MJ, Borgwardt S, et al. (2020): Prevention of Psychosis: Advances in Detection, Prognosis, and Intervention. *JAMA Psychiatry*. 77:755-765.
20. Atkinson RJ, Michie PT, Schall U (2012): Duration mismatch negativity and P3a in first-episode psychosis and individuals at ultra-high risk of psychosis. *Biol Psychiatry*. 71:98-104.
21. Carrion RE, Cornblatt BA, McLaughlin D, Chang J, Auther AM, Olsen RH, et al. (2015): Contributions of early cortical processing and reading ability to functional status in individuals at clinical high risk for psychosis. *Schizophr Res*. 164:1-7.
22. Hsieh MH, Shan JC, Huang WL, Cheng WC, Chiu MJ, Jaw FS, et al. (2012): Auditory event-related potential of subjects with suspected pre-psychotic state and first-episode psychosis. *Schizophr Res*. 140:243-249.
23. Jahshan C, Cadenhead KS, Rissling AJ, Kirihara K, Braff DL, Light GA (2012): Automatic sensory information processing abnormalities across the illness course of schizophrenia. *Psychol Med*. 42:85-97.
24. Kim M, Lee TH, Yoon YB, Lee TY, Kwon JS (2018): Predicting Remission in Subjects at Clinical High Risk for Psychosis Using Mismatch Negativity. *Schizophr Bull*. 44:575-583.
25. Koshiyama D, Kirihara K, Tada M, Nagai T, Koike S, Suga M, et al. (2017): Duration and frequency mismatch negativity shows no progressive reduction in early stages of psychosis. *Schizophr Res*. 190:32-38.

26. Lavoie S, Jack BN, Griffiths O, Ando A, Amminger P, Couroupis A, et al. (2018): Impaired mismatch negativity to frequency deviants in individuals at ultra-high risk for psychosis, and preliminary evidence for further impairment with transition to psychosis. *Schizophr Res*. 191:95-100.
27. Murphy JR, Rawdon C, Kelleher I, Twomey D, Markey PS, Cannon M, et al. (2013): Reduced duration mismatch negativity in adolescents with psychotic symptoms: further evidence for mismatch negativity as a possible biomarker for vulnerability to psychosis. *BMC Psychiatry*. 13:45.
28. Pantlin LN, Davalos D (2016): Neurophysiology for Detection of High Risk for Psychosis. *Schizophr Res Treatment*. 2016:2697971.
29. Perez VB, Woods SW, Roach BJ, Ford JM, McGlashan TH, Srihari VH, et al. (2014): Automatic auditory processing deficits in schizophrenia and clinical high-risk patients: forecasting psychosis risk with mismatch negativity. *Biol Psychiatry*. 75:459-469.
30. Shaikh M, Valmaggia L, Broome MR, Dutt A, Lappin J, Day F, et al. (2012): Reduced mismatch negativity predates the onset of psychosis. *Schizophr Res*. 134:42-48.
31. Shin KS, Kim JS, Kang DH, Koh Y, Choi JS, O'Donnell BF, et al. (2009): Pre-attentive auditory processing in ultra-high-risk for schizophrenia with magnetoencephalography. *Biol Psychiatry*. 65:1071-1078.
32. Solis-Vivanco R, Mondragon-Maya A, Leon-Ortiz P, Rodriguez-Agudelo Y, Cadenhead KS, de la Fuente-Sandoval C (2014): Mismatch Negativity reduction in the left cortical regions in first-episode psychosis and in individuals at ultra high-risk for psychosis. *Schizophr Res*. 158:58-63.
33. Valt C, Quarto T, Tavella A, Romanelli F, Fazio L, Arcara G, et al. (2022): Reduced magnetic mismatch negativity: a shared deficit in psychosis and related risk. *Psychol Med*.1-9.
34. Nagai T, Tada M, Kirihara K, Yahata N, Hashimoto R, Araki T, et al. (2013): Auditory mismatch negativity and P3a in response to duration and frequency changes in the early stages of psychosis. *Schizophr Res*. 150:547-554.
35. Fujioka M, Kirihara K, Koshiyama D, Tada M, Nagai T, Usui K, et al. (2020): Mismatch Negativity Predicts Remission and Neurocognitive Function in Individuals at Ultra-High Risk for Psychosis. *Front Psychiatry*. 11:770.
36. Tateno T, Higuchi Y, Nakajima S, Sasabayashi D, Nakamura M, Ueno M, et al. (2021): Features of Duration Mismatch Negativity Around the Onset of Overt Psychotic Disorders: A Longitudinal Study. *Cereb Cortex*. 31:2416-2424.
37. Wu G, Tang X, Gan R, Zeng J, Hu Y, Xu L, et al. (2022): Automatic auditory processing features in distinct subtypes of patients at clinical high risk for psychosis: Forecasting remission with mismatch negativity. *Hum Brain Mapp*. 43:5452-5464.
38. Shin KS, Kim JS, Kim SN, Koh Y, Jang JH, An SK, et al. (2012): Aberrant auditory processing in schizophrenia and in subjects at ultra-high-risk for psychosis. *Schizophr Bull*. 38:1258-1267.
39. Kim M, Kim T, Hwang WJ, Lho SK, Moon SY, Lee TY, et al. (2023): Forecasting prognostic trajectories with mismatch negativity in early psychosis. *Psychol Med*. 53:1489-1499.
40. Atkinson RJ, Fulham WR, Michie PT, Ward PB, Todd J, Stain H, et al. (2017): Electrophysiological, cognitive and clinical profiles of at-risk mental state: The longitudinal Minds in Transition (MinT) study. *PLoS One*. 12:e0171657.
41. Brockhaus-Dumke A, Tendolkar I, Pukrop R, Schultze-Lutter F, Klosterkotter J, Ruhrmann S (2005): Impaired mismatch negativity generation in prodromal subjects and patients with schizophrenia. *Schizophr Res*. 73:297-310.
42. Hirt V, Schubring D, Schalinski I, Rockstroh B (2019): Mismatch negativity and cognitive performance in the course of schizophrenia. *Int J Psychophysiol*. 145:30-39.
43. Lepock JR, Ahmed S, Mizrahi R, Gerritsen CJ, Maheandiran M, Drvaric L, et al. (2020): Relationships between cognitive event-related brain potential measures in patients at clinical high risk for psychosis. *Schizophr Res*. 226:84-94.
44. Mondragon-Maya A, Solis-Vivanco R, Leon-Ortiz P, Rodriguez-Agudelo Y, Yanez-Tellez G, Bernal-Hernandez J, et al. (2013): Reduced P3a amplitudes in antipsychotic naive first-episode psychosis patients and individuals at clinical high-risk for psychosis. *J Psychiatr Res*. 47:755-761.
45. Bodatsch M, Ruhrmann S, Wagner M, Muller R, Schultze-Lutter F, Frommann I, et al. (2011): Prediction of psychosis by mismatch negativity. *Biol Psychiatry*. 69:959-966.
46. Hamilton HK, Roach BJ, Bachman PM, Belger A, Carrión RE, Duncan E, et al. (2022): Mismatch negativity in response to auditory deviance and risk for future psychosis in youth at clinical high risk for psychosis. *JAMA psychiatry*. 79:780-789.
47. Higuchi Y, Sumiyoshi T, Seo T, Miyanishi T, Kawasaki Y, Suzuki M (2013): Mismatch negativity and cognitive performance for the prediction of psychosis in subjects with at-risk mental state. *PLoS One*. 8:e54080.
48. Naatanen R, Shiga T, Asano S, Yabe H (2015): Mismatch negativity (MMN) deficiency: a break-through biomarker in predicting psychosis onset. *Int J Psychophysiol*. 95:338-344.

49. Javitt DC, Lee M, Kantrowitz JT, Martinez A (2018): Mismatch negativity as a biomarker of theta band oscillatory dysfunction in schizophrenia. *Schizophr Res*. 191:51-60.
50. Fuentemilla L, Marco-Pallares J, Munte TF, Grau C (2008): Theta EEG oscillatory activity and auditory change detection. *Brain Res*. 1220:93-101.
51. Lakatos P, O'Connell MN, Barczak A, McGinnis T, Neymotin S, Schroeder CE, et al. (2020): The Thalamocortical Circuit of Auditory Mismatch Negativity. *Biol Psychiatry*. 87:770-780.
52. Lee M, Sehatpour P, Hoptman MJ, Lakatos P, Dias EC, Kantrowitz JT, et al. (2017): Neural mechanisms of mismatch negativity dysfunction in schizophrenia. *Mol Psychiatry*. 22:1585-1593.
53. Uhlhaas PJ, Gajwani R, Gross J, Gumley AI, Lawrie SM, Schwannauer M (2017): The Youth Mental Health Risk and Resilience Study (YouR-Study). *BMC Psychiatry*. 17:43.
54. McDonald M, Christoforidou E, Van Rijsbergen N, Gajwani R, Gross J, Gumley AI, et al. (2019): Using online screening in the general population to detect participants at clinical high-risk for psychosis. *Schizophrenia Bulletin*. 45:600-609.
55. Schultze-Lutter F, Addington, J., Ruhrmann, S., Klosterkötter, K. (2007): *SCHIZOPHRENIA PRONENESS INSTRUMENT, ADULT VERSION (SPI-A)*. Rome: Giovanni Fioriti Editore
56. First MB, Williams JB, Karg RS, Spitzer RL (2015): Structured clinical interview for DSM-5—Research version (SCID-5 for DSM-5, research version; SCID-5-RV). *Arlington, VA: American Psychiatric Association*.1-94.
57. Kay SR, Fiszbein A, Opler LA (1987): The positive and negative syndrome scale (PANSS) for schizophrenia. *Schizophr Bull*. 13:261-276.
58. Keefe RS, Goldberg TE, Harvey PD, Gold JM, Poe MP, Coughenour L (2004): The Brief Assessment of Cognition in Schizophrenia: reliability, sensitivity, and comparison with a standard neurocognitive battery. *Schizophr Res*. 68:283-297.
59. Hansen P, Kringelbach M, Salmelin R (2010): *MEG: An introduction to methods*. Oxford university press.
60. Besl P, McKay H (1992): A method for registration of 3-D shapes. *IEEE Transactions on pattern analysis and machine intelligence*. 14:239-256.
61. Tzourio-Mazoyer N, Landeau B, Papathanassiou D, Crivello F, Etard O, Delcroix N, et al. (2002): Automated anatomical labeling of activations in SPM using a macroscopic anatomical parcellation of the MNI MRI single-subject brain. *Neuroimage*. 15:273-289.
62. Rinne T, Alho K, Ilmoniemi RJ, Virtanen J, Naatanen R (2000): Separate time behaviors of the temporal and frontal mismatch negativity sources. *Neuroimage*. 12:14-19.
63. Opitz B, Rinne T, Mecklinger A, von Cramon DY, Schroger E (2002): Differential contribution of frontal and temporal cortices to auditory change detection: fMRI and ERP results. *Neuroimage*. 15:167-174.
64. Doeller CF, Opitz B, Mecklinger A, Krick C, Reith W, Schroger E (2003): Prefrontal cortex involvement in preattentive auditory deviance detection: neuroimaging and electrophysiological evidence. *Neuroimage*. 20:1270-1282.
65. Sarvas J (1987): Basic mathematical and electromagnetic concepts of the biomagnetic inverse problem. *Phys Med Biol*. 32:11-22.
66. Salisbury DF, Polizzotto NR, Nestor PG, Haigh SM, Koehler J, McCarley RW (2017): Pitch and Duration Mismatch Negativity and Premorbid Intellect in the First Hospitalized Schizophrenia Spectrum. *Schizophr Bull*. 43:407-416.
67. Magno E, Yeap S, Thakore JH, Garavan H, De Sanctis P, Foxe JJ (2008): Are auditory-evoked frequency and duration mismatch negativity deficits endophenotypic for schizophrenia? High-density electrical mapping in clinically unaffected first-degree relatives and first-episode and chronic schizophrenia. *Biol Psychiatry*. 64:385-391.
68. Umbricht DS, Bates JA, Lieberman JA, Kane JM, Javitt DC (2006): Electrophysiological indices of automatic and controlled auditory information processing in first-episode, recent-onset and chronic schizophrenia. *Biol Psychiatry*. 59:762-772.
69. Salisbury DF, Shenton ME, Griggs CB, Bonner-Jackson A, McCarley RW (2002): Mismatch negativity in chronic schizophrenia and first-episode schizophrenia. *Arch Gen Psychiatry*. 59:686-694.
70. Valkonen-Korhonen M, Purhonen M, Tarkka IM, Sipila P, Partanen J, Karhu J, et al. (2003): Altered auditory processing in acutely psychotic never-medicated first-episode patients. *Brain Res Cogn Brain Res*. 17:747-758.
71. Haigh SM, Coffman BA, Salisbury DF (2017): Mismatch Negativity in First-Episode Schizophrenia: A Meta-Analysis. *Clin EEG Neurosci*. 48:3-10.
72. Kaur M, Battisti RA, Ward PB, Ahmed A, Hickie IB, Hermens DF (2011): MMN/P3a deficits in first episode psychosis: comparing schizophrenia-spectrum and affective-spectrum subgroups. *Schizophr Res*. 130:203-209.
73. Oades RD, Wild-Wall N, Juran SA, Sachsse J, Oknina LB, Ropcke B (2006): Auditory change detection in schizophrenia: sources of activity, related neuropsychological function and symptoms in patients with a first episode in adolescence, and patients 14 years after an adolescent illness-onset. *BMC Psychiatry*. 6:7.

74. Salisbury DF, Kuroki N, Kasai K, Shenton ME, McCarley RW (2007): Progressive and interrelated functional and structural evidence of post-onset brain reduction in schizophrenia. *Arch Gen Psychiatry*. 64:521-529.
75. Grent-'t-Jong T, Gajwani R, Gross J, Gumley AI, Krishnadas R, Lawrie SM, et al. (2021): 40-Hz Auditory Steady-State Responses Characterize Circuit Dysfunctions and Predict Clinical Outcomes in Clinical High-Risk for Psychosis Participants: A Magnetoencephalography Study. *Biol Psychiatry*. 90:419-429.
76. Grent T, Gajwani R, Gross J, Gumley AI, Krishnadas R, Lawrie SM, et al. (2020): Association of magnetoencephalographically measured high-frequency oscillations in visual cortex with circuit dysfunctions in local and large-scale networks during emerging psychosis. *JAMA psychiatry*. 77:852-862.
77. Fusar-Poli P, Schultze-Lutter F (2016): Predicting the onset of psychosis in patients at clinical high risk: practical guide to probabilistic prognostic reasoning. *Evid Based Ment Health*. 19:10-15.
78. Fusar-Poli P, Schultze-Lutter F, Cappucciati M, Rutigliano G, Bonoldi I, Stahl D, et al. (2016): The Dark Side of the Moon: Meta-analytical Impact of Recruitment Strategies on Risk Enrichment in the Clinical High Risk State for Psychosis. *Schizophr Bull*. 42:732-743.
79. Fusar-Poli P, Cappucciati M, Rutigliano G, Schultze-Lutter F, Bonoldi I, Borgwardt S, et al. (2015): At risk or not at risk? A meta-analysis of the prognostic accuracy of psychometric interviews for psychosis prediction. *World Psychiatry*. 14:322-332.
80. Radua J, Ramella-Cravaro V, Ioannidis JP, Reichenberg A, Phiphopthatsanee N, Amir T, et al. (2018): What causes psychosis? An umbrella review of risk and protective factors. *World psychiatry*. 17:49-66.
81. Haining K, Matrunola C, Mitchell L, Gajwani R, Gross J, Gumley AI, et al. (2020): Neuropsychological deficits in participants at clinical high risk for psychosis recruited from the community: relationships to functioning and clinical symptoms. *Psychological medicine*. 50:77-85.

Figure Legends

Figure 1: Experimental Paradigm and Regions of Interest

A) Task paradigm showing standard sequences, duration deviant and omission sequences. B) Source-localized, whole-brain areas of evoked responses during duration deviant MMNm across all participants. Colour indicates t-values, false discovery rate–corrected brain activity. C) Location of virtual electrodes used for group differences - Heschl's Gyrus (HES) and Superior Temporal Gyrus (STG) bilaterally.

Figure 2. ERF-Responses in Auditory Cortex

Event related fields (ERFs) computed on time series extracted from virtual electrodes placed in bilateral auditory cortices for different participant groups. In each subpanel, first vertical line marks the onset of first tone in the sequence at 0 ms while second vertical line marks the onset of the last tone at 600 ms; the dotted vertical lines mark the time window where the duration deviant Mismatch Negativity (MMN) was identified (765 to 785 ms). Top row - Left Heschl's Gyrus (LHES); second row - Left Superior Temporal Gyrus (LSTG); third row - Right Heschl's Gyrus (RHES); bottom row - Right Superior Temporal Gyrus (RSTG); Leftmost column – Healthy Controls (HC); second column – Clinically High-Risk Negative (CHR-N); third column – Clinically High Risk for Psychosis (CHR-P); rightmost column – First Episode Psychosis (FEP) groups.

Figure 3. Time Frequency Analysis in Auditory Cortex

Time frequency decomposition: spectral power and Inter Trial Phase Coherence (ITPC) of time series extracted from virtual electrodes placed in bilateral auditory cortices for different participant groups. In each subpanel, first vertical line marks the onset of first tone in the sequence at 0 ms while second vertical line marks the onset of the last tone at 600 ms; in spectrograms white horizontal lines mark the theta band (4-8 Hz). Top row - Left Heschl's Gyrus (LHES); second row - Left Superior Temporal Gyrus (LSTG); third row - Right Heschl's Gyrus (RHES); bottom row - Right Superior Temporal Gyrus (RSTG); Leftmost column – Time frequency decomposition results from Healthy Controls (HC); second column – Time frequency decomposition in theta band from all 4 sub-groups: HC, Clinically High Risk Negative (CHR-N), Clinically

High Risk for Psychosis (CHR-P), First Episode Psychosis (FEP) patients; third column – ITPC from Healthy Controls; rightmost column – ITPC results in theta band from all 4 sub-groups: HC, CHR-N, CHR-P, FEP

Table 1 Demographics, Clinical Data, and Task Performance

Characteristics	**HC**	**CHR-N**	**CHR-P**	**FEP**	**Group effect** [a]	**Post Hoc comparisons**
Number of participants	49	38	116	33	–	–
Age, years, mean (SD)	23 (3.6)	23 (4.7)	22 (4.5)	24 (4.5)	$H_3 = 10.1$, $p = .018$	FEP > CHR-P: $p = .015$
Sex, male/female, n (% male)	16/33 (32.7%)	11/27 (28.9%)	34/82 (29.3%)	22/11 (66.7%)	$\chi^2_3 = 16.9$, $p = .001$	FEP > HC: $p = .002$ FEP > CHR-N: $p = .001$ FEP > CHR-P: $p < .001$
Education, years, mean (SD)	17 (3.0)	16 (3.5)	15 (3.2)	15 (2.8)	$H_3 = 9.9$, $p = .019$	CHR-P < HC: $p = .032$
BACS, Mean (SD) [b]						
Verbal memory	52 (8.7)	0.01 (1.1)	−0.36 (1.3)	NA	–	–
Digit sequencing	21 (2.1)	0.14 (1.2)	−0.16 (1.5)	NA	–	–
Token motor	81 (11.6)	−0.66 (1.1)	−1.01 (1.3)	NA	$H_2 = 20.7$, $p < .001$	CHR-P < HC: $p < .001$
Verbal fluency	59 (13.9)	−0.22 (1.0)	0.05 (1.3)	NA	–	–
Symbol coding	74 (11.8)	0.00 (1.3)	−0.58 (1.1)	NA	$H_2 = 15.8$, $p < .001$	CHR-P < HC: $p = .002$ CHR-P < CHR-N: $p = .013$
Tower of London	19 (1.7)	0.15 (1.3)	−0.15 (1.5)	NA	–	–
Composite score	304 (24.2)	−0.15 (1.2)	−0.62 (1.4)	NA	$H_2 = 9.6$, $p = .008$	CHR-P < HC: $p = .014$
CAARMS, Mean (SD)						
Unusual thought content	0 (0.1)	1 (1.2)	2 (2.0)	NA	–	–
Non-bizarre ideas	0 (0.4)	1 (1.1)	3 (1.8)	NA	–	–
Perceptual abnormalities	0 (0.5)	1 (1.3)	3 (1.5)	NA	–	–
Disorganized speech	0 (0.1)	1 (0.9)	1 (1.4)	NA	–	–
Total severity score	1 (2.4)	6 (6.1)	30 (18.0)	NA	$H_2 = 125.2$, $p < .001$	CHR-N > HC: $p = .01$ CHR-P > HC: $p < .001$ CHR-P > CHR-N: $p < .001$
GAF, mean (SD)	88 (6.4)	70 (12.8)	58 (13.8)	39 (13.7)	$H_2 = 140.8$, $p < .001$	All contrasts $p < .005$
GF Role, mean (SD)	8.6 (0.8)	8.1 (0.8)	7.4 (1.2)	NA	$H_2 = 50.5$, $p < .001$	CHR-P < HC: $p < .001$

Characteristics	HC	CHR-N	CHR-P	FEP	Group effect [a]	Post Hoc comparisons
						CHR-P < CHR-N: p = .002
GF Social, mean (SD)	8.8 (0.4)	8.2 (0.8)	7.4 (1.3)	NA	H_2 = 62.0, p < .001	CHR-N < HC: p = .003 CHR-P < HC: p < .001 CHR-P < CHR-N: p = .003
Medication, n (%) [c]						
None	48 (98%)	27 (71%)	60 (52%)	14 (42%)	–	–
Antidepressants	0	11 (29%)	46 (40%)	15 (45%)	–	–
Mood stabilizers	0	0	5 (4%)	0	–	–
Antipsychotics	0	0	2 (2%)	18 (55%)	–	–
Other	1 (2%)	2 (5%)	17 (15%)	7 (21%)	–	–
MEG Trials, Total Included, Mean (SD)	217.2 (12.8)	219.2 (16)	214.8 (15.1)	215.8 (9.8)	H = 1.01, p < .39	
Task Performance						
Accuracy, %	97.4% (2.2%)	97.4% (2.9%)	95.8% (6%)	95.2% (5.7%)	H = 2.47, p < .063	
False alarm %	3.6% (1.4%)	3.7% (1.2%)	4.5% (3.7%)	4.5% (1.8%)	H = 1.72, p < .163	

HC – Healthy Controls group; CHR-N – Clinically High Risk Negative group; CHR-P – Clinically High Risk for Psychosis group; FEP – First Episode Psychosis patients; SD – standard deviation

a - Except for sex statistical testing, which are based on χ2 tests, all other tests are based on nonparametric Kruskal-Wallis H-tests: α = 0.05, two-sided, adjusted for ties, post hoc Bonferroni-corrected for multiple comparisons.

b - BACS scores for clinical groups were standardized to control group data, controlled for sex.

c - Multiple categories possible.

Table 2 FEP-Specific Clinical Data

Psychopathology	FEP
PANSS, Mean (SD)	
Positive	20 (8.0)
Negative	16 (9.2)
Cognitive	21 (9.2)
Excitement	9 (4.5)
Depression	11 (5.8)

Psychopathology	**FEP**
Total score	77 (28.3)
DSM-5/SCID-IP, n	
Schizophrenia	10
Schizophreniform disorder	3
Schizoaffective disorder	1
Psychotic disorder NOS	13
Brief psychotic disorder	1
Mood disorders with psychotic symptoms	4
Delusional disorder	1

FEP, first-episode psychosis; NOS, not otherwise specified; PANSS, Positive and Negative Syndrome Scale; SCID-IP, Structured Clinical Interview for DSM-5 Axis I Disorders-Patient Edition.

Table 3 CHR- and HC-Specific Clinical Data

Characteristics	**HC**	**CHR-N**	**CHR-P**
CHR-P Categories			
SPI-A, n (%) [COGDIS/COPER/both items]	0	0	30 (26%) [4/15/11]
CAARMS, n (%) [APS-/GRFD-criteria]	0	0	31 (27%) [29/2]
CAARMS+SPI-A, n (%) [COGDIS/COPER/both items]	0	0	55 (47%) [8/22/25]
SPI-A Severity, Mean (SD)	0	0	11 (11.6)
MINI Categories, n (%)*			
Depressive/mood disorders	0 (0%)	11 (29%)	75 (65%)
Anxiety disorders/PTSD/OCD	0 (0%)	16 (42%)	85 (73%)
Drug/alcohol abuse/dependence	2 (4%)	10 (26%)	39 (33%)
Eating disorders	0 (0%)	1 (2%)	9 (8%)

* Multiple categories possible for comorbidities.

APS, attenuated psychotic symptom; CAARMS, Comprehensive Assessment of At-Risk Mental States; CHR-N, Clinical High Risk Negative group; CHR-P, Clinical High Risk for Psychosis group; COGDIS, Cognitive Disturbances; COPER, Cognitive-Perceptive basic symptoms criterion; GRFD, genetic risk and functional decline; HC, healthy control; MINI, Mini-International Neuropsychiatric Interview; OCD, obsessive-compulsive disorder; PTSD, posttraumatic stress disorder; SPI-A, Schizophrenia Proneness Instrument, Adult version.

Table 4 Virtual electrode - ERF, theta band spectral power enhancement, theta band ITPC enhancement - statistical results in the entire group

ROI	Main effect of group statistics on virtual electrodes					
	ERF		Theta band power		Theta band ITPC	
	F(3,232)	p-value	F(3,232)	p-value	F(3,232)	p-value
Left HES	*1.088*	*0.36*	*0.19*	*0.9*	*0.49*	*0.69*
Left STG	*0.79*	*0.5*	*0.43*	*0.73*	*1.17*	*0.32*
Right HES	*0.0287*	*0.99*	*0.67*	*0.57*	*0.71*	*0.54*
Right STG	*0.115*	*0.95*	*0.36*	*0.78*	*0.33*	*0.8*

HES – Heschl's Gyrus; STG – Superior Temporal Gyrus; ERF – Evoked Response Field; Theta band 4-8 Hz; ITPC – Inter Trial Phase Coherence; * - denotes significance after correcting for multiple comparisons.

A)

B)

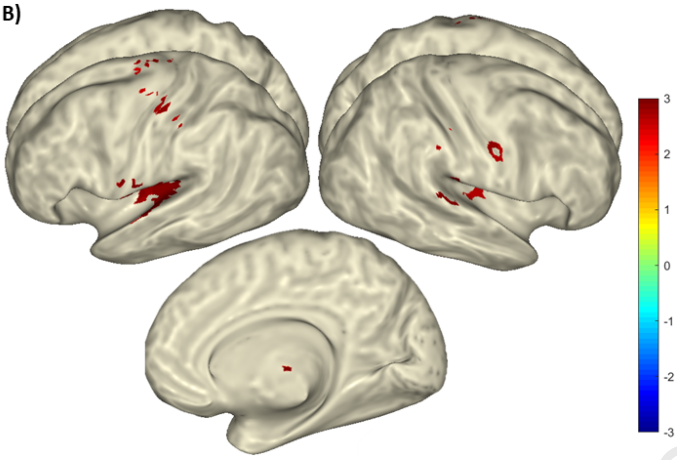

C)